Addendum to *Powered Flight*

Bonus Material

Ch. 6:

6.1) p. 181, for further clarification on compression and heating, add the following near the end of first paragraph:

A single axial compressor stage (rotor + stator) would typically give a compression ratio of up to 2:1, and with many stages possible, one can presently deliver up to 40:1 overall compression.

As a general rule-of-thumb, one can assume that each stage in a given compressor has the same temperature rise (ΔT). Therefore, as the entry temperature ($T_{stage\ entry}$) to each stage must increase progressively through the compressor, the ratio $\Delta T/T_{stage\ entry}$ must decrease, thus implying a progressive reduction in stage pressure ratio through the unit. Hence, the rearmost stage develops a significantly lower pressure ratio than the first stage. This also applies to radial compressor stages.

6.2) pp. 183-184, for further info, can add the following diagram and text:

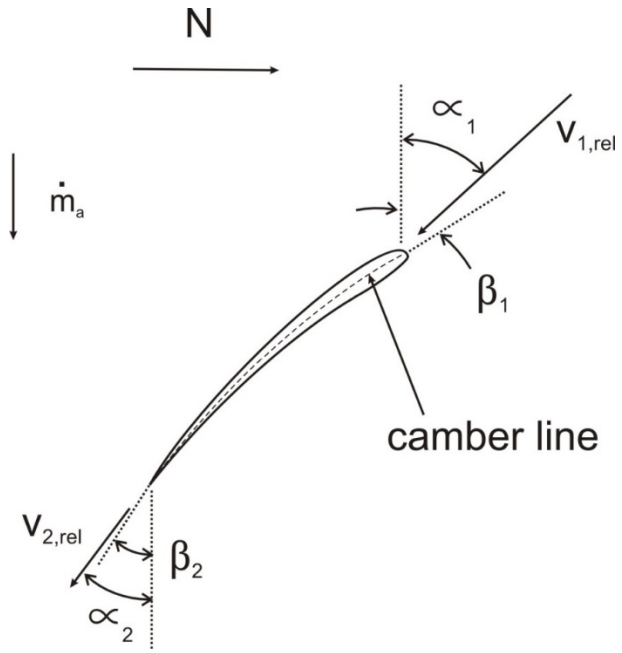

Blade geometry with respect to leading edge and trailing edge angles illustrated above. Here, define α as air angle relative to the longitudinal axis, β as blade angle (camber line relative to longitudinal axis).

Define incidence angle as $\beta_1 - \alpha_1$ and deviation angle as $\alpha_2 - \beta_2$. Define deflection angle as $\alpha_1 - \alpha_2$, and camber as $\beta_1 - \beta_2$.

These velocity triangles help to establish the resultant flow direction and effective angle of attack α of a given airfoil section. From an analytical viewpoint, one can apply a momentum-blade element approach for estimating the lift, drag and resulting torque acting on a given blade, as done earlier for a propeller blade.

Ch. 10:

10.1) pp. 330-331, more info on SRM combustion processes below:

Thermal decompostion (endothermic process: requires heat input to system) of AP (ammonium perchlorate), example products of reaction for balanced equilibrium concentrations:

$$2NH_4ClO_4(\text{solid}) + \text{heat} \rightarrow 2O_2(\text{gas}) + N_2(g) + 4H_2O(g) + Cl_2(g)$$

In practice, decomposition products would also include transitional and equilibrium quantities of $HClO_4$, NH_3 , CO_2 , OH , CO , HCl , H_2 , etc.

Thermal decomposition of HTPB may be approximated via:

$$HO(C_4H_4)_{50}OH(s) + \text{heat} \rightarrow 49C_4H_4(g) + 2CO(g) + C_2H_6(g)$$

where C_4H_4 = cyclobutadiene

Combustion of HTPB decomposition products with surrounding hot gas, with exothermic heat release and example products of reaction for balanced equilibrium concentrations:

$$C_4H_4(g) + 5O_2(g) \rightarrow 4CO_2(g) + 2H_2O(g) + \text{heat}$$

As per the previous reactions, O_2 as a reactant provided from the decomposition of AP.

Combustion of aluminum with surrounding hot gas, example products of reaction for balanced equilibrium concentrations:

$$4Al(s) + 3O_2(g) \rightarrow 2Al_2O_3(s) + heat$$

$$2Al(s) + 3Cl_2(g) \rightarrow 2AlCl_3(g) + heat$$

Assuming a general reaction process with exothermic heat output, for AP and aluminum as reactants:

$$6NH_4ClO_4(s) + 10Al(s) \rightarrow 4Al_2O_3(s) + 2AlCl_3(g) + 3N_2(g) + 12H_2O + heat$$

where $AlCl_3$ = alum. chloride, Al_2O_3 = alum. oxide

Ch. 12:

12.1) p. 421, for further clarification on empirical coefficient *a,* as per the port diameter d_p correction used in the Lenoir-Robillard model's erosive burning component for SRMs, p. 335, Eq. (10.8), one can say the following then for *a* (to be used for the axial-dependent burning law for HREs):

$$a = a_{ref}(d_p^{0.2})_{ref} / (d_p^{0.2})$$

For example, if one wished to use the empirical law for HRE burning (Eq. 12.1), one might attain better accuracy when using a value for coefficient a_{ref} from another source by noting the corresponding approx. value for port diameter $d_{p,\,ref}$ that produced that value for a_{ref} , and in turn apply the above correction to give the updated *a* at the new d_p (or range of values thereof for the new case).

12.2) p. 422, further to the above port diameter correction on coeff. *a*, as to its effect on Eq. (12.4), one would get the following alternate result:

$$\text{Mass flow of fuel} = K_1 \cdot d^{0.8-2n}$$

Hence, in this case, for n > 0.4 (rather than 0.5), one would see a decrease in mass flow of fuel as time progressed into an HRE firing, and port diameter increasing.

12.3) p.419, can include the following note in regards to oxidizer injection:

Potential flame stability upper limit issue on incoming G_0 , e.g., 350 kg/m^2-s for liquid oxidizer, and 700 kg/m^2-s for gaseous oxidizer entry; flame will blow out if mass flux too high above these nominal limit values from past conventional flame blowout studies.

12.4) p. 421, effect of swirl in increasing HRE fuel regression rate, can include the following diagrams laying out how one might model the flow physics of swirl (head-end oxidizer injection at a swirl angle):

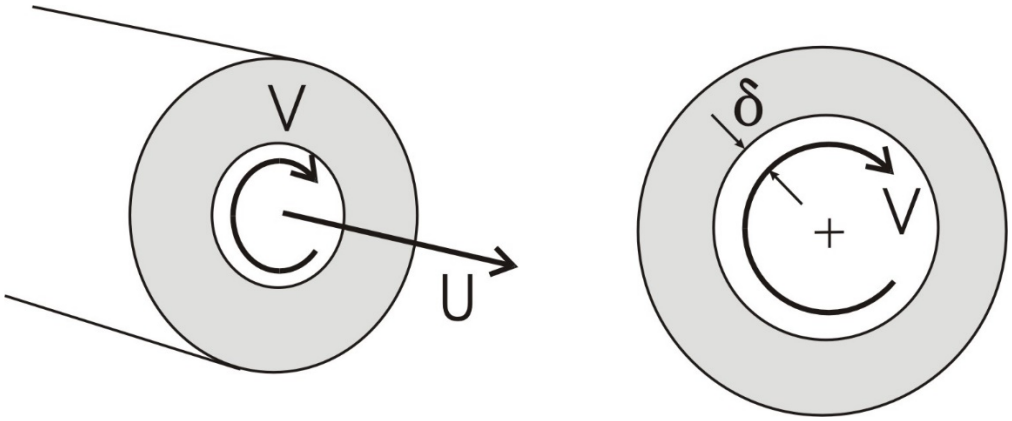

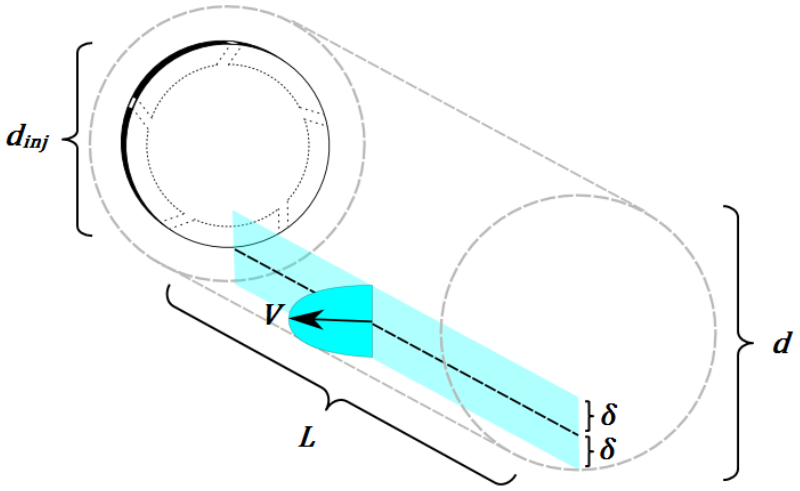

See the following article for further info: Wongyai, P. and Greatrix, D.R., "Regression Rate Estimation for Swirling-Flow Hybrid Rocket Engines," *Journal of Propulsion & Power*, Vol. 32, No. 1, Jan.-Feb. 2016, pp. 18-22.

12.5) p. 417, sample info on combustion process for a paraffin/N_2O engine setup, noting solid paraffin wax as a fuel is comparable performance-wise to liquid kerosene, and burns significantly faster than conventional plastic fuels like PE, or rubber fuels like HTPB:

Equilibrium chemical reaction between nitrous oxide and paraffin wax may be approximated by the following:

$$85N_2O(g) + C_{28}H_{58}(s) \rightarrow 85N_2(g) + 29H_2O(g) + 28CO_2(g) + \text{heat}$$

12.6) pp. 427-429, further info on HRE combustion instability below:

- Susceptible to both axial and transverse symptoms in the combustor (pressure waves); higher frequencies more damaging than lower frequencies, at high wave amplitudes
- At low wave frequencies (LF), one can observe symptoms of significant amplitude associated with feed system instability (related to injectors and upstream plumbing); also TCG (thermal lag/combustion/gasdynamic) intrinsic instability
- Cold outside air temperatures tend to cause instability issues

- Based on thermal lag/combustion/ gasdynamic (TCG) response of processes occurring at low frequency in the combustion chamber, Karabeyoglu derived the following empirical relation to give the associated TCG frequency (aka, intrinsic LF frequency):

$$f_{LF} = 0.234[\,2 + 1/\,r\,]\,\frac{4}{\pi}\,\frac{\dot{m}_o RT_{av}}{L \cdot p \cdot d_p^2}$$

where T_{av} is the average gas temp., R is the specific gas constant, L is eff. chamber length, r is O/F ratio. Ranges in value from 5 to 50 Hz. Small RU-PRF HRE, LF value predicted to be around 20 Hz.

- Based on a simple idealized chamber filling-emptying cycle, the following formula, derived at Ryerson University PRF in 2017, looks promising as an alternative, less empirical formula for estimating the intrinsic LF frequency:

$$f_{LF} = \frac{0.5}{c^*} \frac{A_t}{A_p} \frac{RT_{av}}{L}$$

Small RU-PRF HRE, LF value predicted by above eqn. to be around 25 Hz.

Low Freq. Z-N response, low-r_b HRE (ATK 1995 engine; firing simulation, 2015 RU-PRF project):

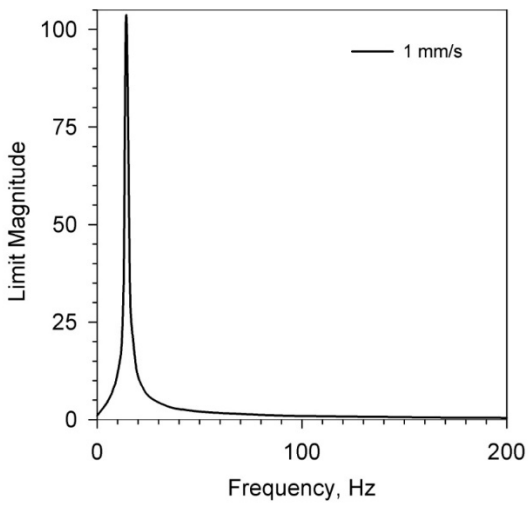

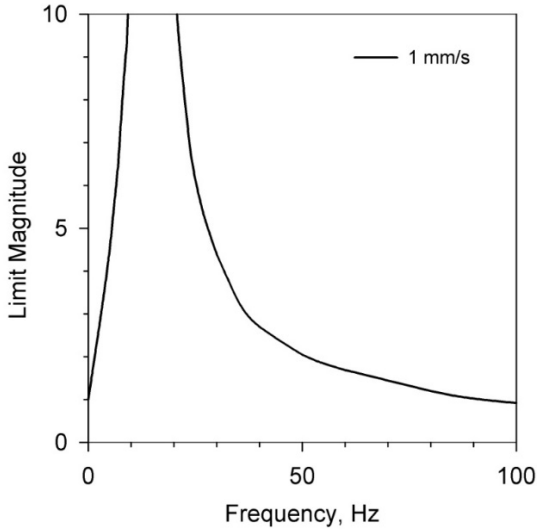

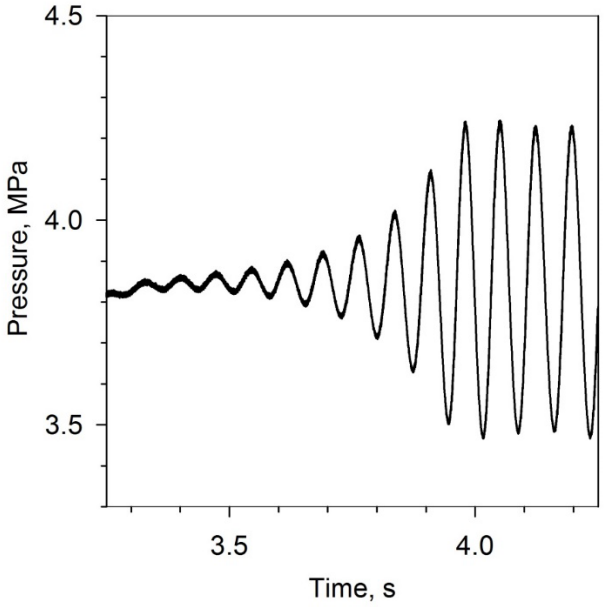

Head-end pressure-time profile, ATK (Boardman et al.,1995) engine, 13-Hz LF oscillation; HRE firing simulation: $K_b = 550\ s^{-1}$, $\Delta H_{S,ZN} = +215{,}000$ J/kg, $r_o = 1$ mm/s

Acoustic (higher frequency, HF) combustion instability:

- occasionally, one might observe 1L (fundamental axial) pressure waves present in the combustion chamber… while typically of lower magnitude relative to LF waves, the higher 1L frequency can introduce the potential for some deleterious effects on the rocket engine and flight vehicle
- mechanism for 1L activity to date regarded as "unknown" , although influences such as thermal lag occasionally quoted; 2017 work at RU suggests radial vibrational acceleration of fuel surface, and corresponding transient augmented burning rate locally, sufficient to support this axial pressure wave activity, possibly in combination with a HF Z-N influence (2016 RU study)

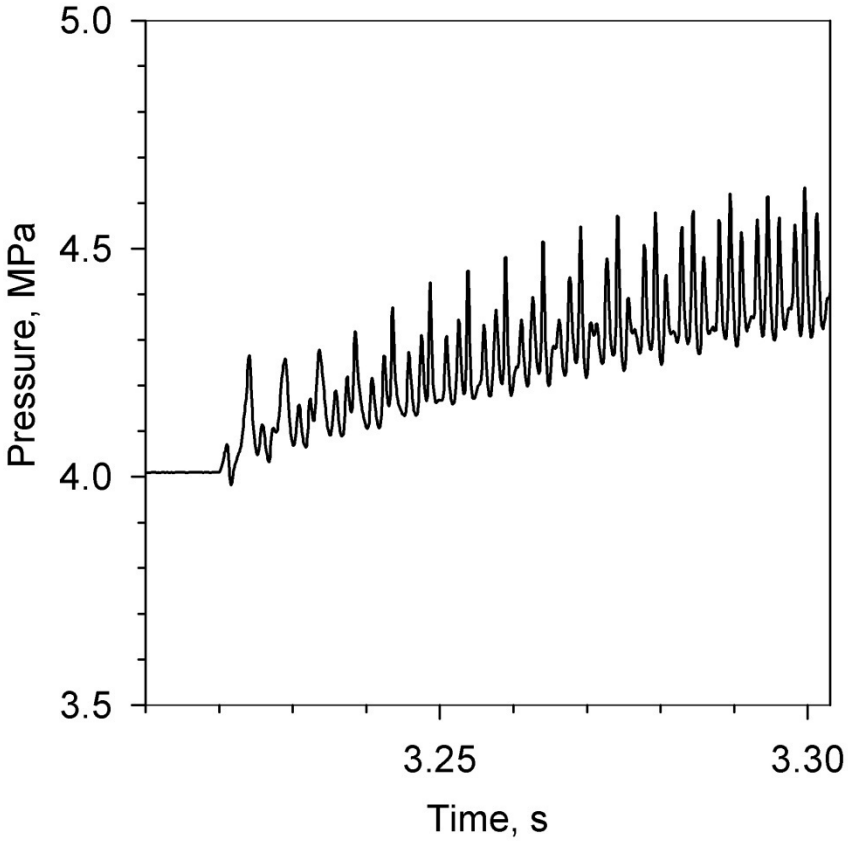

1L axial frequency approx. 180 Hz, dc shift of 0.3 MPa, 0.35 MPa peak sustained axial pressure wave magnitude due to radial vibration (no Z-N influence included in this RU-PRF simulation for head-end pressure vs. time; 2017 project)

Reference:

Greatrix, D.R., "LF and HF Combustion Instability in Hybrid Rocket Engines," AIAA/ASME/SAE/ASEE 54th Joint Propulsion Conference, AIAA Paper No. 2018- 4527, Cincinnati, July 9 – 11, 2018.